Metrics other than potency reveal systematic variation in responses to cancer drugs

Mohammad Fallahi-Sichani[1], Saman Honarnejad[1], Laura M Heiser[2], Joe W Gray[2] & Peter K Sorger[1]*

Large-scale analysis of cellular response to anticancer drugs typically focuses on variation in potency (half-maximum inhibitory concentration, (IC$_{50}$)), assuming that it is the most important difference between effective and ineffective drugs or sensitive and resistant cells. We took a multiparametric approach involving analysis of the slope of the dose-response curve, the area under the curve and the maximum effect (E_{max}). We found that some of these parameters vary systematically with cell line and others with drug class. For cell-cycle inhibitors, E_{max} often but not always correlated with cell proliferation rate. For drugs targeting the Akt/PI3K/mTOR pathway, dose-response curves were unusually shallow. Classical pharmacology has no ready explanation for this phenomenon, but single-cell analysis showed that it correlated with significant and heritable cell-to-cell variability in the extent of target inhibition. We conclude that parameters other than potency should be considered in the comparative analysis of drug response, particularly at clinically relevant concentrations near and above the IC$_{50}$.

Patient-to-patient variability in drug response is a primary challenge facing development and use of new medicines[1]. A recent approach to understanding such variability involves genotyping coupled with systematic measurement of dose-response across a large and diverse bank ('encyclopedia') of cell lines[2–8]. In the case of anticancer drugs that block cell proliferation or induce apoptosis[9], cells are typically exposed to drug over a 10^4- to 10^5-fold concentration range, and viability is measured after 72–96 h. Such data is conventionally analyzed from the perspective of IC$_{50}$ values (or similar parameters), which are descriptive of the shape of the dose-response curve at its midpoint. However, inspection of dose-response curves reveals that they differ substantially in shape from one drug to the next and from one cell line to the next. Variability in shape can be quantified by performing a multiparametric analysis using a conventional logistical sigmoidal function

$$y = E_{inf} + \left(\frac{E_0 - E_{inf}}{1 + \left(\dfrac{D}{EC_{50}} \right)^{HS}} \right) \quad (1)$$

where y is a response measure at dose D (typically the experimental data), E_0 and E_{inf} are the top and bottom asymptotes of the response, EC$_{50}$ is the concentration at half-maximal effect, and Hill slope (HS) is a slope parameter analogous to the Hill coefficient[10–12] (**Fig. 1a**). Three values derived from equation (1) are in common use: IC$_{50}$, E_{max} and the area under the dose-response curve (AUC). Although they are not strictly parameters of equation (1), we refer to E_{max}, IC$_{50}$ and AUC as 'parameters' for simplicity. EC$_{50}$ and IC$_{50}$ are the classic measures of drug potency, and E_{max} and E_{inf} are measures of drug efficacy (for anticancer drugs, E_{max} varies between 1 at low doses and 0 at high doses, which corresponds to death of all of the cells). AUC combines potency and efficacy of a drug into a single parameter. AUC values can be compared for a single drug across multiple cell lines exposed to the same range of drug concentrations, but comparison of different drugs is problematic (because the scaling between drugs and dose ranges is generally

arbitrary). In the simple case of second-order competitive inhibition, the case considered in most pharmacology textbooks, $E_0 = 1$, $E_{max} = E_{inf} = 0$, EC$_{50}$ = IC$_{50}$ and HS = 1 (**Fig. 1a**).

The focus to date on potency[2–4,6–8,13] ignores the potential impact and biological importance of variation in other parameters, such as the steepness of the dose-response curve or differences in maximum effect (although one recent large-scale study did compute E_{max} and AUC[5]). In this paper, we show that different dose-response parameters encode distinct information; some parameters varied systematically with cell line and others with drug. For example, HS and E_{max} were frequently uncorrelated with each other or with half-maximum growth inhibition (GI$_{50}$), but the parameters varied in a consistent way within a drug class. Because the origins of systematic variation in HS and E_{max} are poorly understood, we performed single-cell analysis of Akt/PI3K/mTOR inhibitors and found that cell-to-cell variability is one explanation for shallow dose-response relationships. Thus, multiparametric analysis yields insight into understudied aspects of drug response that are particularly important near and above the IC$_{50}$ value, a concentration range relevant to human patients.

RESULTS

Dose-response parameters vary with compound and cell line

We focused on analysis of previously published data comprising CellTiter-Glo measurement of per-well ATP concentrations (a metric of metabolically active cells)[14] for 64 anticancer drugs (**Supplementary Results**, **Supplementary Table 1**) and 53 well-characterized breast cell lines[3]. Assays were performed before and 3 d after exposure to drugs at nine doses spanning a ~10^5-fold range (with maximum doses between 0.5 μM and 20 mM depending on potency[3]). We computed viability as $y = N/N_C$, where the cell number N was measured in the presence of drug, and cell number N_C is measured in a no-drug control. As the number of cells present before the start of the experiment was available (N_0), we also computed $y^* = (N - N_0)/(N_C - N_0)$ to yield the GI$_{50}$ value for $y^* = 0.5$ (**Fig. 1b**). We confirmed key findings using independent dose-response data released through the Cancer Cell Line Project (for which estimates of N_0 are not available)[4].

[1]Harvard Medical School Library of Integrated Network-based Cellular Signatures Center, Department of Systems Biology, Harvard Medical School, Boston, Massachusetts, USA. [2]Department of Biomedical Engineering, Oregon Health and Science University, Portland, Oregon, USA.
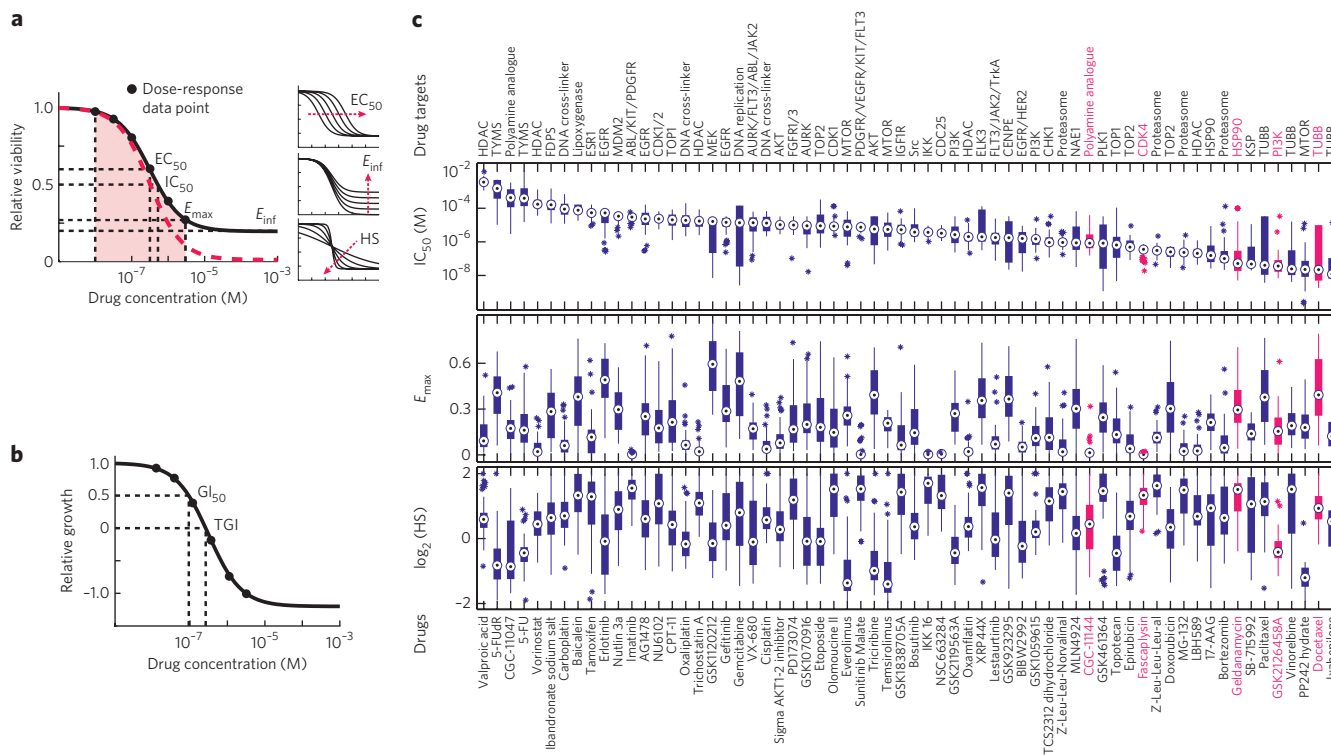*e-mail: peter_sorger@hms.harvard.edu

Figure 1 | Diversity of anticancer compounds with respect to variation in dose-response parameters across a panel of breast cell lines. (**a**) Schematic of key dose-response parameters (EC_{50}, IC_{50}, E_{inf}, E_{max} and AUC) calculated following curve fitting to the cell survival data. The pink area represents the AUC. The red dashed line represents the simple case of $E_0 = 1$, $E_{max} = E_{inf} = 0$, $EC_{50} = IC_{50}$ and HS = 1. Effects of variations in EC_{50}, slope (HS) and E_{inf} on the shape of dose-response curve are shown on the right; details of parameters and logistic equation are described in the text. (**b**) Schematic of key dose-response parameters (GI_{50} and total growth inhibition (TGI)) that can be calculated by fitting logistic curves to data on relative cell growth comprising a change in cell number after drug treatment normalized to the change in cell number in an untreated control well. (**c**) The range of dose-response parameters, IC_{50} (a measure of potency), E_{max} (a measure of efficacy) and HS (a measure of curve steepness) estimated for all 64 compounds across all 53 of the breast cell lines are represented by box-and-whisker plots and median parameter values and interquartile ranges; bars extending to 1.5× the interquartile range are shown for each drug as a measure of variance. Parameter values for outlier cell lines are marked with asterisks. Compounds are sorted on the basis of the median IC_{50} value. Drug targets are nominal and do not include off-target effects.

Multiparametric analysis yielded values for EC_{50}, IC_{50}, GI_{50}, HS, E_{inf}, E_{max} and AUC for 2,789 drug–cell line combinations (**Supplementary Data Set 1**; http://lincs.hms.harvard.edu/db/datasets/20120/; data filtering described in Online Methods) and revealed substantial differences from one drug and cell line to the next (**Fig. 1c**). For example, across cell lines, IC_{50} varied ~10^4-fold, and E_{max} varied from 0 to 0.8 for the microtubule stabilizer docetaxel and HSP90 inhibitor geldanamycin (**Fig. 2a,b**), whereas IC_{50} varied little for the CDK4/cyclin D1 kinase inhibitor

fascaplysin (no more than tenfold), and the maximum effect was high in all cases (E_{max} ~0; **Fig. 2c**). In the case of the PI3K inhibitor GSK2126458, the HS was ~1.0, whereas it varied substantially for the polyamine analog CGC-11144 (**Fig. 2d,e**).

Association of maximal effect parameters with cell type

We observed that potency, maximal effect and slope were well correlated only for a subset of drugs and cell lines (**Fig. 3a** and **Supplementary Fig. 1**). For example, whereas IC_{50} and E_{max}
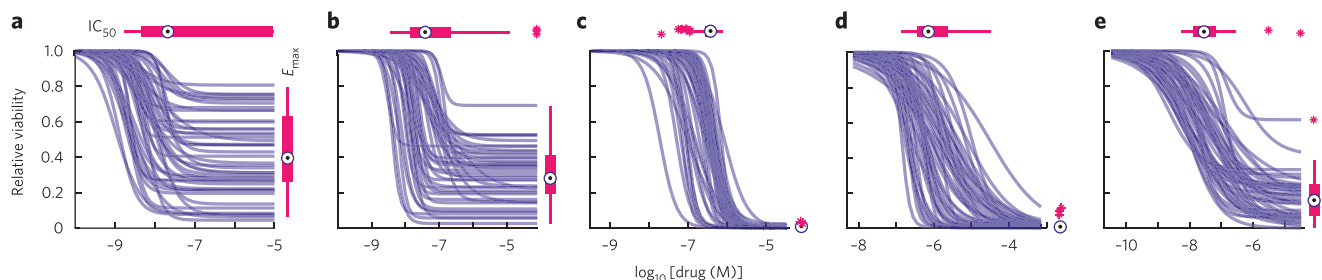

Figure 2 | Selected examples of dose-response curves representing different types of variation in dose-response relationships. (**a–e**) Patterns of dose response across the breast cell line panel for docetaxel, a microtubule stabilizer (**a**); geldanamycin, an HSP90 inhibitor (**b**); fascaplysin, a CDK4 inhibitor (**c**); CGC-11144, a polyamine analog (**d**); and GSK2126458, a PI3K inhibitor (**e**), are shown. These drugs are highlighted in magenta in **Figure 1c**. The range of IC_{50} and E_{max} values is represented by box-and-whisker plots, and median parameter values and interquartile ranges are shown above and to the right; bars extending to 1.5× the interquartile range are shown for each drug as a measure of variance. Parameter values for outlier cell lines are denoted by stars.
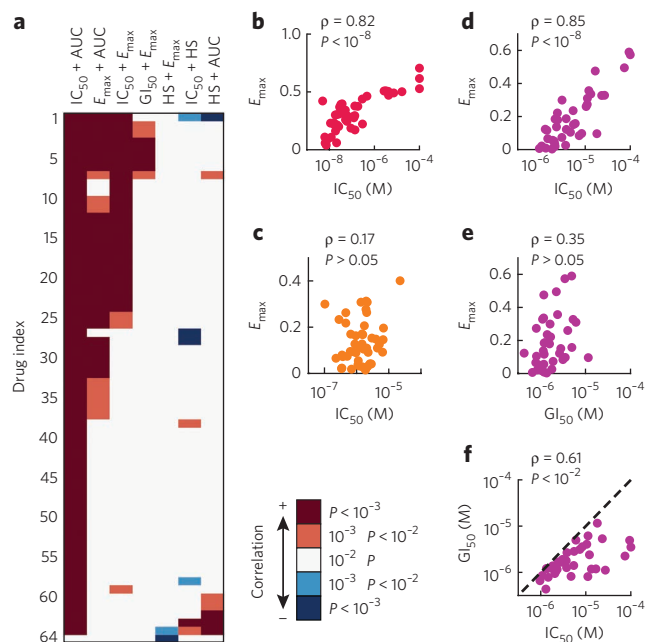
709

Figure 3 | Different dose-response parameters do not always correlate with each other. (**a**) Pairwise correlation between different key dose-response parameters estimated for each drug across the breast cancer cell line collection. *P* values were corrected using the Bonferroni-Holm method. A complete view of the graph, including drug names corresponding to each drug index, is presented in **Supplementary Figure 1**. Correlation coefficient values and corrected *P* values are presented in **Supplementary Data Set 3**. (**b**,**c**) Pairwise distribution and correlation of E_{max} and IC_{50} for geldanamycin (an HSP90 inhibitor) (**b**) and GSK1059615 (a PI3K inhibitor) (**c**). (**d**–**f**) Pairwise distribution and correlation of E_{max} and IC_{50} (**d**), E_{max} and GI_{50} (**e**) and IC_{50} and GI_{50} (**f**) for bosutinib (a Src/Abl inhibitor) across the cell line panel. Each circle represents a cell line. Colors represent different drugs.

correlated in the case of geldanamycin, they did not for the PI3K inhibitor GSK1059615 (**Fig. 3b,c**). IC_{50} and E_{max} were generally more highly correlated than GI_{50} and E_{max} (for example, for the Src/Abl inhibitor bosutinib: $P = 10^{-11}$ versus $P = 0.03$; **Fig. 3d–f**). Thus, parameters we might assume to be interchangeable (for example, IC_{50} and GI_{50}) were not, implying that different dose-response parameters convey different information. To quantify this, we computed the mutual information (MI)[15] between parameter values and either cell or drug type. MI is an information theoretic metric that reveals how informative one variable (for example, IC_{50} or E_{max}) is about a second variable (for example, drug identity or cell type). For example, an MI score of 0 bits for a parameter-drug pair means that they are independent, whereas a score of 1 bit means pairs can be divided into $2^1 = 2$ groups having either a low or a high parameter value; similarly, a score of 1.6 bits implies division into $2^{1.6} \approx 3$ groups. We estimated the probabilities of observing different values of each dose-response parameter for all of the compounds and cell lines and used MI *P* values as a statistical measure of significance (this is necessary because nonzero MI values are expected by chance for randomly permuted data). We computed empirical *P* values by randomly shuffling the dose-response data ($n = 10,000$) across all of the cell lines and drugs (further details are in Online Methods).

Parameters quantifying maximum effect (E_{max} and E_{inf}) showed strong association ($P < 10^{-4}$) with cell type. For example, all but three of the drugs had an equal or higher value for E_{max} in SKBR3 cells than in SUM159PT cells (**Fig. 4a**). IC_{50} had a weaker association ($P = \sim 0.05$) with cell type and EC_{50}, and HS had no significant association (**Supplementary Table 2**). Prevailing 'fractional kill'
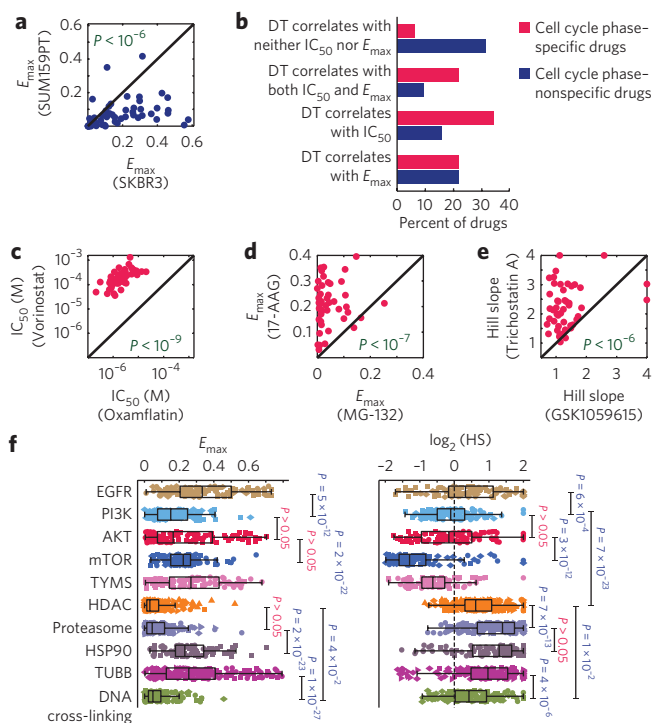

Figure 4 | Association of dose-response parameters with cell type, drug type and drug class. (**a**) An example showing that two cell lines (SUM159PT and SKBR3) are distinguishable by E_{max} values, with SUM159PT cells having lower values for all but three compounds. Significance of difference between the E_{max} values for the two cell lines was evaluated by *P* value based on a nonparametric Wilcoxon signed-rank test. (**b**) Correlation between different dose-response parameters estimated for the set of anticancer compounds and the doubling times across the breast cell lines. Drugs are grouped in two groups: drugs specific and nonspecific for cell cycle phase. The complete list of drugs in each group is in **Supplementary Figure 2**. The percentage of drugs within each group that show a significant correlation ($P < 0.05$) between doubling time (DT) and parameters E_{max} and IC_{50} is shown. *P* values were corrected using the Benjamini-Hochberg method. Correlation coefficient values and corresponding *P* values are presented in **Supplementary Data Set 4**. (**c**–**e**) Three examples of anticancer drugs that are distinguishable on the basis of dose-response parameter values across the breast cell line panel as discovered by mutual information analysis: vorinostat and oxamflatin (**c**), 17-AAG and MG-132 (**d**), trichostatin A and GSK1059615 (**e**). The significance of differences between drugs was evaluated by *P* values based on a nonparametric Wilcoxon signed-rank test. (**f**) Variation of E_{max} and HS for different classes of drugs defined on the basis of target or mechanism of action across the breast cell lines. Significance of differences between drug classes was evaluated by *P* values based on a nonparametric Mann-Whitney *U*-test and was corrected using the Bonferroni-Holm method.

theory[16,17] posits that inhibitors of cell-cycle progression (such as paclitaxel) kill only the subset of cells that pass through S or M phases in the presence of drug. Consistent with this, SKBR3 had a substantially longer doubling time than SUM159PT cells (~50 h versus ~20 h and thus lower mitotic and S phase fractions) under the growth conditions used in this study. When we calculated the correlation between dose-response parameters and cell doubling time for all 64 drugs, we observed a strong positive correlation between E_{max} or IC_{50} and doubling time, particularly in the case of DNA-damaging agents and microtubule stabilizers (**Fig. 4b** and **Supplementary Fig. 2**). However, when we excluded nominally cell cycle–specific drugs from the analysis (**Supplementary Fig. 2**),
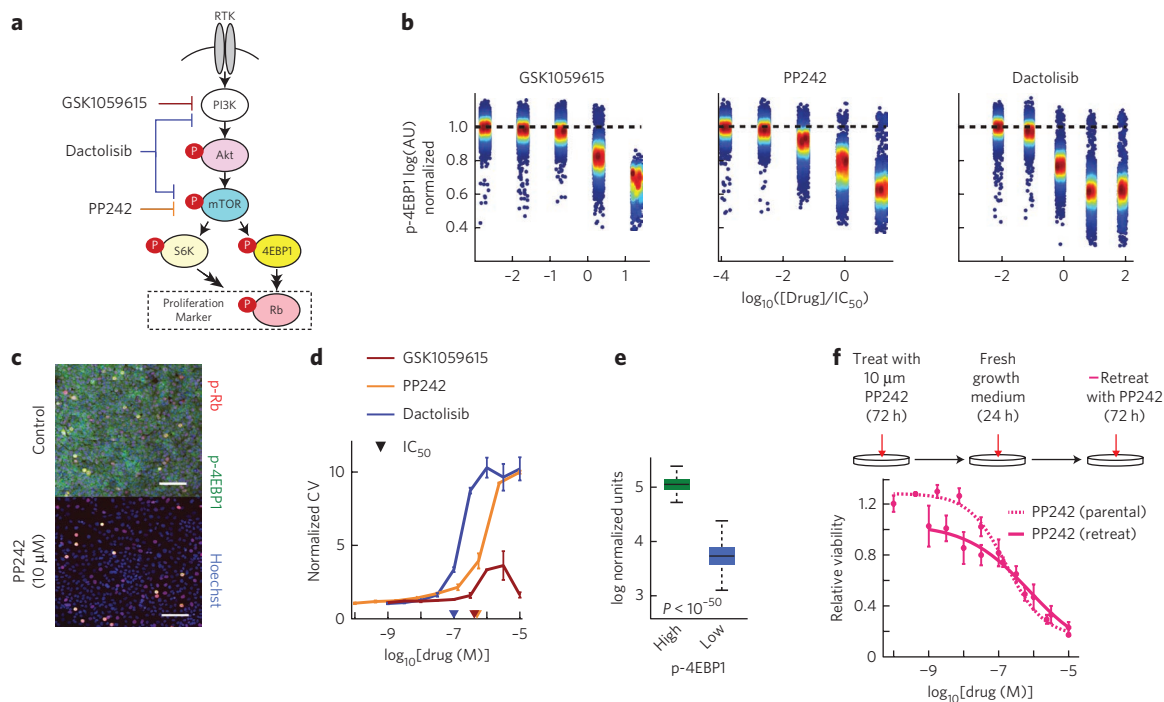
Figure 5 | High cell-to-cell variability is associated with shallow dose-response and suboptimal maximum effect for pharmacological inhibition of mTOR. (a) PI3K/Akt/mTOR pathway and its associated downstream effectors. Highly simplified schematic showing how drug response was assessed by measuring amounts of phosphorylated Akt (p-Akt), S6 ribosomal protein, 4EBP1 and Rb on the single-cell level by immunofluorescence microscopy. **(b)** Dose-dependent inhibition of p-4EBP1 in MCF10A cells with increasing drug concentrations, as illustrated by intensity values on a single-cell basis. **(c)** Selected immunofluorescence images of p-4EBP1, p-Rb and Hoechst staining of MCF10A cells in the absence of drug and 24 h after exposure to 10 μM PP242. Scale bars represent 100 μm. **(d)** The effect of GSK1059615, PP242 and dactolisib on coefficient of variation (the s.d. for single-cell measurements divided by the population average) of single-cell amounts of p-4EBP1. Data represent mean values ± s.d. calculated from two replicates per dose of drug. **(e)** Cells with high p-4EBP1 (cells with p-4EBP1 amounts above that of the population average) 24 h after exposure to 10 μM PP242 have >10× larger amounts of p-Rb than cells with low p-4EBP1 (cells with p-4EBP1 amounts below that of the population average). Median p-Rb signal intensities and interquartile ranges and bars extending to 1.5× the interquartile range are shown. **(f)** Retreating surviving MCF10A cells (exposure to 10 μM PP242 for 72 h followed by fresh growth medium for 24 h) with nine doses of PP242 for 72 h results in a shallow dose-response curve with similar dose-response parameters as those observed for parental cells.

the association between cell line and both E_{max} and E_{inf} was still statistically significant ($P = ~0.02$), albeit weaker. Moreover, drugs not classically considered to be inhibitors of cell cycle processes had E_{max} values that correlated with proliferation rate; in the case of bortezomib, the correlation might reflect the role of the proteasome in degradation of cyclins, p21 and p27 (refs. 18–20), but this is less obvious in the case of drugs such as the HSP90 inhibitor geldanamycin. Also unexpected was the observation that E_{max} values for some cell-cycle inhibitors did not correlate with proliferation rate. For example, the CDK4 inhibitor fascaplysin, the CDC25 inhibitor NSC663284 and the DNA cross-linking agents cisplatin, carboplatin and oxaliplatin all had an E_{max} of ~0 in most cell lines, and any variation was independent of proliferation rate.

Association of E_{max} and HS with drug class

We observed a strong association ($P < 10^{-4}$) between drug type and potency, efficacy and steepness of the dose-response relationships (**Supplementary Table 2**), meaning that virtually all of the drug pairs could be distinguished on the basis of cell line–dependent variation in one or more parameters. For example, the parameters IC_{50}, E_{max} and HS allowed high-confidence ($P = 10^{-9}$ to 10^{-6}) discrimination between the pairs of drugs (i) oxamflatin and vorinostat (two HDAC inhibitors), (ii) MG-132 (a proteasome inhibitor) and 17-AAG (an HSP90 inhibitor), and (iii) GSK1059615 (a PI3K inhibitor) and trichostatin A (an HDAC inhibitor) (**Fig. 4c–e**). Distinguishability by IC_{50} is intuitively obvious and arises when the

affinity of a drug for its target is greater than that of a second drug for its target, making the first compound universally more potent.

To better understand distinguishability by parameters other than potency, we grouped drugs into classes on the basis of nominal target or mechanism of action (ignoring potential secondary targets and polypharmacology). We subjected dose-response data for different drug classes to principal component analysis (PCA; **Supplementary Fig. 3**) to rotate the data into a new principal component space in which relationships between dose-response parameters and target could be visualized (independent of cell line). We found that drugs from the same class usually clustered together (**Supplementary Fig. 3**). For example, HDAC inhibitors, proteasome inhibitors and DNA cross-linking drugs had uniformly high maximal effects ($E_{max} \sim E_{inf} \sim 0$), whereas inhibitors of EGFR and HSP90 had large variation in E_{max} (**Fig. 4f**). In the case of HS, mTOR inhibitors had $\overline{HS} \approx 0.41$ (with a median absolute deviation of 0.11), and for pyrimidine analog or thymidylate synthase inhibitors, $\overline{HS} \approx 0.65$ (median absolute deviation = 0.15). These values were significantly less than one ($P < 1 \times 10^{-8}$), whereas values of $\overline{HS} \approx 1.5$ to 2.6 for HDAC and proteasome inhibitors were significantly greater than one ($P < 1 \times 10^{-13}$). Cooperativity is the usual explanation for HS > 1 in classical enzymology and pharmacology, and the steep dose-response curve for proteasome inhibitors is presumed to reflect the presence of seven catalytic subunits in the active enzyme[21]. However, situations in which HS < 1 are less commonly considered, and neither sequential nor independent binding schemes with negative cooperativity result in HS < 1 (ref. 22).

We confirmed that HS varied with drug class using the Cancer Cell Line Project data set, which covers 639 human cell lines and 130 drugs[4]. The published data comprise concentration values at different fractional effect size (that is, EC$_{25}$, EC$_{50}$, EC$_{75}$ and EC$_{90}$), and we therefore approximated HS by the EC$_{25}$/EC$_{75}$ ratio (**Supplementary Data Set 2**). Among the 40 breast cancer lines in this data set, we found that EGFR inhibitors had significantly higher HS values than PI3K inhibitors ($P = 9 \times 10^{-6}$), and PI3K and AKT inhibitors had higher HS values than mTOR inhibitors ($P = \sim10^{-5}$–10^{-4}), whereas HDAC and proteasome inhibitors had significantly higher HS values than all three classes of drugs ($P = 10^{-3}$ to 10^{-8}); this was also true when we examined all of the cell lines in the Cancer Cell Line Project data set (**Supplementary Fig. 4**). We conclude that HS varies in a consistent way with drug class across multiple data sets.

Cell-to-cell variability and shallow dose-response curves

To investigate how a shallow dose-response curve might arise, we focused on drugs inhibiting the PI3K/Akt/mTOR pathway that varied widely in HS and E_{max} values, independent of proliferation rate. As a class, these drugs are undergoing extensive clinical investigation[23], with more than 300 trials at http://www.ClinicalTrials.gov/. For three compounds with varying HS, we measured target inhibition by immunofluorescence microscopy and cell killing in four breast cell lines (HER2-amplified AU565 and HCC1954 cancer cells, hormone receptor–positive T47D cancer cells and nontransformed MCF10A cells). We probed the effects of the mTOR inhibitor PP242, the PI3K inhibitor GSK1059615 and the dual-specificity mTOR/PI3K inhibitor dactolisib (BEZ235) 24 h after drug exposure in nine-point dose-response assays using antibodies specific for phospho-Akt (p-Akt; at Ser473), p-4EBP1 (at Thr37 and Thr46) and p-S6 (at Ser235 and Ser236) (**Fig. 5a**); p-4EBP1 in particular is generally considered to be the most informative downstream marker of Akt/mTOR/PI3K pathway activity[24,25]. We also measured amounts of p-Rb (at Ser807 and Ser811) as a surrogate for commitment to the cell cycle[26]. Immunofluorescence microscopy revealed dose-dependent inhibition of p-Akt, p-4EBP1 and p-S6 (**Supplementary Fig. 5**), and viability assays performed 72 h after drug exposure confirmed that HS << 1 for PP242 and dactolisib and HS ~1 for GSK1059615 in all of the cell lines (**Supplementary Fig. 6**). However, we also observed substantial cell-to-cell variability in phospho-protein staining intensity for cells exposed to the first two drugs (**Fig. 5b,c**): the coefficient of variation in p-4EBP1 staining (that is, the s.d. of immunofluorescence signal intensity at the single-cell level divided by the population average) rose for cells treated with PP242 or dactolisib near the IC$_{50}$ but not for GSK1059615, which had a low and constant coefficient of variation (**Fig. 5d**). We observed similar results for other cell lines (**Supplementary Figs. 7–9**). We conclude that a shallow dose-response curve is correlated with high cell-to-cell variability in target inhibition compared to drugs for which HS ~ 1 (in four of four cell lines tested).

Even at the highest drug concentrations tested (10 μM), a fraction of cells exposed to PP242 but not GSK1059615 retained high p-4EBP1 staining (**Fig. 5b,c**). The outlier population in PP242-treated cells with high p-4EBP1 staining had approximately ten-fold higher p-Rb staining ($P < 10^{-50}$) compared to the population with low p-4EBP1, implying that outliers were committed to cell proliferation (**Fig. 5e**). The presence of a subset of cells in which the Akt/mTOR/PI3K pathway is insensitive to inhibition by PP242 or dactolisib is a likely explanation for fractional cell killing by these drugs ($E_{max} > 0$). To determine whether these insensitive cells represent a stable subpopulation or whether they interconvert with sensitive cells, we exposed cultures to two successive drug treatments. We treated MCF10A cells with PP242 for 72 h at a concentration (10 μM) sufficient to induce apoptosis or block
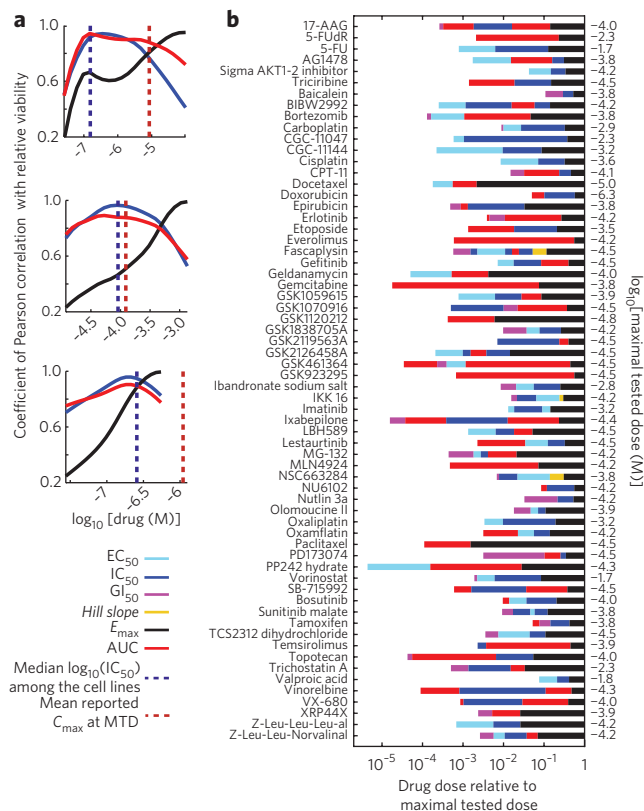
proliferation in ~80% of cells. We exchanged the medium and allowed viable cells to recover for 24 h before being exposed a second time to PP242 at a range of nine doses (1 nM to 10 μM) for 72 h. When we compared dose-response curves for the parental (drug-naive) and survivor cell populations (**Fig. 5f**), IC$_{50}$ values (~1 μM) and HS < 1 were indistinguishable, showing that drug-sensitive cells can arise rapidly from relatively insensitive cells. Thus fractional response did not reflect the presence of a stable subpopulation of drug-insensitive cells but rather showed rapid interconversion between resistant and sensitive states. Cell-to-cell variability in response to PP242 and the shallow dose-response curve it generates therefore seemed to be stable properties of cell populations.

Variation of cell line responsiveness to each drug class

The value of any single parameter as an effective descriptor of cellular response to a class of drugs should depend on how well the parameter correlates across cell lines. We computed a similarity

Figure 6 | Different dose-response parameters capture cell line to cell line variation at different dose regimes. (**a**) Variations of the predictive value (coefficient of Pearson correlation with relative viability) for each of the three key dose-response parameters (IC$_{50}$, E_{max} and AUC) with dose for three selected drugs, 17-AAG (top), carboplatin (middle) and doxorubicin (bottom). (**b**) Predictive value of different dose-response parameters for drug sensitivity is a function of the clinical concentration of drug. Dose-response parameters corresponding to the most significant correlation (as evaluated by P value) with cellular response (that is, relative viability) at doses spanning a range from the IC$_{50}$ of the most sensitive cell line to the highest tested dose for each drug are shown. For example, for the mTOR inhibitor PP242, EC$_{50}$ (denoted by light blue bar) is the parameter with the highest correlation with relative viability when cell lines are exposed to drug concentrations around 10^{-5} times the maximal tested dose (that is, $10^{-5} \times 10^{-4.3}$ M ≈ 0.5 nM). At a 100-fold higher concentration (that is, $10^{-3} \times 10^{-4.3}$ M ≈ 50 nM), AUC (denoted by red bar) shows the strongest correlation with relative viability.

score for drugs with related nominal targets and treated as significant only those cases in which variation across cell lines was more highly correlated within a drug class than across drugs randomly selected from multiple classes (as scored by P value; Online Methods and **Supplementary Fig. 10**). For example, in the case of the HDAC inhibitors vorinostat and LBH589, E_{max} values had a high similarity score as they varied in a consistent way (as illustrated by MDAMB134VI and T47D cells in **Supplementary Fig. 10**). For EGFR inhibitors, IC_{50} values were strongly correlated across cell lines (Pearson's correlation coefficient = 0.90, $P < 10^{-7}$ for erlotinib and AG1478), but E_{max} was not correlated (Pearson's correlation coefficient ~0.4, $P \sim 0.1$). The reasons for these differences are not known, but we speculate that erlotinib and AG1478 exert their effects on the same target (EGFR) near their IC_{50} values but have additional and different targets at high drug concentrations where E_{max} values become relevant. When comparing drugs, we must therefore account for the fact that different parameters are informative for different drug classes.

An alternative way to approach this problem is to determine the ability of a single parameter to accurately describe a full dose-response relationship. We computed the correlation between the response estimated from a single parameter of a conventional logistic curve and the measured response. In the case of the canonical dose response having $E_{max} = 0$, $EC_{50} = IC_{50}$ and HS = 1, the correlation would be perfect across all drug concentrations. We performed the analysis across the range of doses for all of the drugs and cell lines by scoring the P values of the correlation coefficient. We observed that E_{max} was best correlated with actual response at high doses, IC_{50} and AUC were best at intermediate doses (near the median IC_{50} for all of the cell lines), and EC_{50} or GI_{50} were best at low doses (near the IC_{50} for the most sensitive cell line). These findings are depicted as continuous plots for 17-AAG, carboplatin and doxorubicin and for the full data set as a set of optimal parameters for each dose range (**Fig. 6a,b**). A priori, we are most interested in parameters that are informative at clinically relevant concentration ranges. We can estimate these ranges from the plasma concentration (C_{max}) at the maximal tolerated dose; in general, effective drugs are ones in which $C_{max}/IC_{50} \gg 1$ (**Supplementary Table 3**). Incorporating this information, we saw that, in the clinical range, the most informative parameter varied with drug (for example, AUC for 17-AAG, IC_{50} for carboplatin and E_{max} for doxorubicin).

DISCUSSION

To date, systematic analysis of large-scale dose-response data has concentrated on the closely related parameters EC_{50}, IC_{50} and GI_{50}, thereby making the implicit assumption that potency at the midpoint of the dose-response curve is the most important difference between drugs or between sensitive and resistant cells[2–4,6–8,13]. In this paper, we examined variation in features other than potency such as E_{max}, HS and AUC. For many drugs, IC_{50} (or GI_{50}), E_{max} and HS did not correlate, and MI analysis revealed systematic variation with both drug and cell type: in the latter case, differences in cell proliferation rates emerged as a probable explanation, particularly for variation in E_{max} and drugs that target cell cycle processes. This is consistent with extensive evidence that inhibitors of DNA synthesis or mitotic spindle assembly exert their effects (at least in culture) only when cells transit S or M phase. However, not all of the cell cycle inhibitors have $E_{max} > 0$. For example, inhibitors of CDK4 (fascaplysin), CDK phosphatase CDC25 (NSC663284) and the DNA cross-linking agents cisplatin, carboplatin and oxaliplatin had $E_{max} \sim 0$ for the vast majority of cell lines tested. Moreover, observed variation in E_{max} was independent of proliferation rate. Conversely, we observed a significant (MI $P < 0.05$) association between E_{max} and proliferation rate for drugs that are not typically considered to be cell cycle inhibitors, including the HSP90

inhibitor geldanamycin and the proteasome inhibitor bortezomib (although the latter drug does affect degradation of cyclins and other cell cycle regulators). Further analysis of killing by cell cycle inhibitors whose effects do and do not correlate with proliferation is likely to be informative, particularly in the case of clinically important cytotoxic chemotherapeutics with similar targets.

For drugs that showed large variation in multiple, uncorrelated dose-response parameters, the question of which one is most informative arose. AUC, a parameter that combines potency and efficacy into a single measure, was robust as a response metric when the goal was to compare a single drug across cell lines exposed to identical dose ranges. Other parameters could be used with multiple drugs and concentration ranges, but their value varied with dose: E_{max} was more informative at high compared to low doses, and the opposite was true of IC_{50} and GI_{50}. With anticancer drugs, it is typical to aim for a maximum serum dose (C_{max}) near the maximum tolerated dose, and drugs for which $C_{max}/IC_{50} \gg$ 1 are preferred clinically. During development of a new drug, reducing IC_{50} is obviously an important goal, but when the aim is to understand variability in patient responses to an existing drug, our data suggest that it is likely to be more informative to focus on E_{max} and HS.

In many cases, the origins of variation in dose-response parameters remain to be determined. Association with drug class or target is confounded by polypharmacology, which almost certainly affects the shape of dose-response curves at high drug concentrations (particularly with phenotypic measures of response). Future analysis of different compounds having the same nominal target should help resolve this issue. Differences in the physicochemistry of drug-target interaction (for example, association rate, polar surface area and so on) are potential sources of variation in parameters other than IC_{50}, and it should be possible to tackle this with sophisticated cheminformatic analysis[27,28]. However, in this paper, we focused on understanding the origins of fractional maximum effect and shallow dose-response curves.

We found that the HS was particularly high for drugs such as proteasome and HDAC inhibitors (for example, bortezomib and LBH589), whereas inhibitors of the Akt/PI3K/mTOR pathway had low and variable HS, particularly drugs such as PP242, temsirolimus, everolimus and rapamycin. Positive cooperativity provides a framework for understanding steep dose-response relationships (HS > 1)[10,22], but even negative cooperativity should not result in HS < 1. By comparing the dose-dependent inhibition of proteins in the Akt/PI3K/mTOR pathway following exposure of cells to drugs with HS ~ 1 or HS < 1, we found that shallow dose response was associated with high cell-to-cell variability in target inhibition. Moreover, when we recovered and expanded cells that were initially insensitive to a drug such as PP242 and then reassayed drug response several days later, we observed the same shallow dose-response curve and fractional killing at high dose as in the original cell population. This implies that HS < 1 is a stable property of a cell population and that states of drug sensitivity and insensitivity interconvert on the timescale of days. We and others have observed similar effects in receptor-mediated cell death[29,30], activation of immune response[31] or sensitivity to chemotherapeutic drugs[32] and ascribed them to stochastic fluctuation in the amounts or activities of intracellular signaling proteins. In principle, the molecules of a drug target present in any single cell could show a canonical HS = 1 dose-response curve, but fluctuation in target amount, activity or interaction with other proteins[33] might cause the IC_{50} value to vary from cell to cell, giving rise to a shallow dose-response curve at the population level.

It is notable that mTOR inhibitors had some of the lowest values for HS and that this pathway is also subject to complex feedback regulation. Moreover, what seem to be static differences from one cell to the next in the fixed-time point experiments in this

paper are likely to arise from temporal fluctuations that are asynchronous across the population. Mutations and nongenetic factors that generate dose-response curves with HS < 1 and $E_{max} > 0$ are likely to be important clinically: the incremental therapeutic benefit of getting closer and closer to the maximum tolerated dose will be less for a drug with a shallow rather than steep dose-response curve. Studies on dose-response relationships for antiviral drugs have also concluded that variation in HS is important for assessing drug sensitivity and resistance[21,34]. Attempts to identify new drugs or effective combination therapies might therefore focus on steepening the dose-response relationship and increasing maximum effect, not just decreasing IC_{50}.

METHODS
Methods and any associated references are available in the online version of the paper.

Accession codes. The authors have deposited the paper's data in the Harvard Medical School Library of Integrated Network-based Cellular Signatures database (http://lincs.hms.harvard.edu/db/datasets/20120/).

References
1. Borden, E.C. & Dowlati, A. Phase I trials of targeted anticancer drugs: a need to refocus. *Nat. Rev. Drug Discov.* **11**, 889–890 (2012).
2. Sos, M.L. *et al.* Predicting drug susceptibility of non–small cell lung cancers based on genetic lesions. *J. Clin. Invest.* **119**, 1727–1740 (2009).
3. Heiser, L.M. *et al.* Subtype and pathway specific responses to anticancer compounds in breast cancer. *Proc. Natl. Acad. Sci. USA* **109**, 2724–2729 (2012).
4. Garnett, M.J. *et al.* Systematic identification of genomic markers of drug sensitivity in cancer cells. *Nature* **483**, 570–575 (2012).
5. Barretina, J. *et al.* The Cancer Cell Line Encyclopedia enables predictive modelling of anticancer drug sensitivity. *Nature* **483**, 603–607 (2012).
6. Greshock, J. *et al.* Molecular target class is predictive of *in vitro* response profile. *Cancer Res.* **70**, 3677–3686 (2010).
7. Solit, D.B. *et al.* BRAF mutation predicts sensitivity to MEK inhibition. *Nature* **439**, 358–362 (2006).
8. Staunton, J.E. *et al.* Chemosensitivity prediction by transcriptional profiling. *Proc. Natl. Acad. Sci. USA* **98**, 10787–10792 (2001).
9. Tyson, D.R., Garbett, S.P., Frick, P.L. & Quaranta, V. Fractional proliferation: a method to deconvolve cell population dynamics from single-cell data. *Nat. Methods* **9**, 923–928 (2012).
10. Hill, A. The possible effects of the aggregation of the molecules of haemoglobin on its dissociation curves. *J. Physiol. (Lond.)* **40**, iv–vii (1910).
11. Chou, T.C. Derivation and properties of Michaelis-Menten type and Hill type equations for reference ligands. *J. Theor. Biol.* **59**, 253–276 (1976).
12. Holford, N.H. & Sheiner, L.B. Understanding the dose-effect relationship: clinical application of pharmacokinetic-pharmacodynamic models. *Clin. Pharmacokinet.* **6**, 429–453 (1981).
13. Shoemaker, R.H. The NCI60 human tumour cell line anticancer drug screen. *Nat. Rev. Cancer* **6**, 813–823 (2006).
14. Hannah, R., Beck, M. & Moravec, R. CellTiter-Glo™ Luminescent cell viability assay: a sensitive and rapid method for determining cell viability. *Promega Cell Notes* **2**, 11–13 (2001).
15. Cover, T.M. & Thomas, J.A. *Elements of Information Theory* (ed. Schilling, D.L.) (John Wiley and Sons, New York, 1991).
16. Berenbaum, M.C. *In vivo* determination of the fractional kill of human tumor cells by chemotherapeutic agents. *Cancer Chemother. Rep.* **56**, 563–571 (1972).
17. Mitchison, T.J. The proliferation rate paradox in antimitotic chemotherapy. *Mol. Biol. Cell* **23**, 1–6 (2012).
18. Glotzer, M., Murray, A.W. & Kirschner, M.W. Cyclin is degraded by the ubiquitin pathway. *Nature* **349**, 132–138 (1991).
19. Aligue, R., Akhavan-Niak, H. & Russell, P. A role for Hsp90 in cell cycle control: Wee1 tyrosine kinase activity requires interaction with Hsp90. *EMBO J.* **13**, 6099–6106 (1994).
20. Bazzaro, M. *et al.* Ubiquitin-proteasome system stress sensitizes ovarian cancer to proteasome inhibitor-induced apoptosis. *Cancer Res.* **66**, 3754–3763 (2006).
21. Shen, L. *et al.* Dose-response curve slope sets class-specific limits on inhibitory potential of anti-HIV drugs. *Nat. Med.* **14**, 762–766 (2008).
22. Weiss, J.N. The Hill equation revisited: uses and misuses. *FASEB J.* **11**, 835–841 (1997).
23. Dancey, J. mTOR signaling and drug development in cancer. *Nat. Rev. Clin. Oncol.* **7**, 209–219 (2010).
24. Hsieh, A.C. *et al.* Genetic dissection of the oncogenic mTOR pathway reveals druggable addiction to translational control via 4EBP-eIF4E. *Cancer Cell* **17**, 249–261 (2010).
25. Feldman, M.E. *et al.* Active-site inhibitors of mTOR target rapamycin-resistant outputs of mTORC1 and mTORC2. *PLoS Biol.* **7**, e38 (2009).
26. Sherr, C.J. Cancer cell cycles. *Science* **274**, 1672–1677 (1996).
27. Keiser, M.J. *et al.* Predicting new molecular targets for known drugs. *Nature* **462**, 175–181 (2009).
28. Lounkine, E. *et al.* Large-scale prediction and testing of drug activity on side-effect targets. *Nature* **486**, 361–367 (2012).
29. Gaudet, S., Spencer, S.L., Chen, W.W. & Sorger, P.K. Exploring the contextual sensitivity of factors that determine cell-to-cell variability in receptor-mediated apoptosis. *PLOS Comput. Biol.* **8**, e1002482 (2012).
30. Spencer, S.L., Gaudet, S., Albeck, J.G., Burke, J.M. & Sorger, P.K. Non-genetic origins of cell-to-cell variability in TRAIL-induced apoptosis. *Nature* **459**, 428–432 (2009).
31. Feinerman, O., Veiga, J., Dorfman, J.R., Germain, R.N. & Altan-Bonnet, G. Variability and robustness in T cell activation from regulated heterogeneity in protein levels. *Science* **321**, 1081–1084 (2008).
32. Cohen, A.A. *et al.* Dynamic proteomics of individual cancer cells in response to a drug. *Science* **322**, 1511–1516 (2008).
33. Sigal, A. *et al.* Variability and memory of protein levels in human cells. *Nature* **444**, 643–646 (2006).
34. Sampah, M.E., Shen, L., Jilek, B.L. & Siliciano, R.F. Dose-response curve slope is a missing dimension in the analysis of HIV-1 drug resistance. *Proc. Natl. Acad. Sci. USA* **108**, 7613–7618 (2011).

Author contributions
M.F.-S. designed and performed the experiments, analyzed the experimental data, performed statistical analyses and wrote the manuscript. S.H. designed and performed the experiments and wrote the manuscript. L.M.H. designed and performed the experiments and wrote the manuscript. J.W.G. designed the experiments and wrote the manuscript. P.K.S. designed the experiments and wrote the manuscript.

Competing financial interests
The authors declare no competing financial interests.

Additional information
Supplementary information is available in the online version of the paper. Reprints and permissions information is available online at http://www.nature.com/reprints/index.html. Correspondence and requests for materials should be addressed to P.K.S.

ONLINE METHODS

Dose-response curve fitting. We obtained dose-response curves for the 72-h effect of 64 drugs, including both targeted agents and cytotoxic therapeutics on the viability and growth of 53 breast cell lines using previously published data[3] (http://lincs.hms.harvard.edu/db/datasets/20120/). Briefly, we fitted triplicate nine-dose (1:5 serial dilution) data to the logistical sigmoidal model (equation (1); constraints: $E_0 = 1$ and $0 < HS < 4$) using nonlinear least-squares regression performed in GraphPad Prism 6. We excluded 'no response' data defined as data that (i) showed higher statistical quality (based on extra-sum-of-squares F test) when fitted to a constant model ($y = E_{inf}$) in comparison with the sigmoidal model or (ii) their sigmoidal fitted curve Hill slopes were < 0.25, from the analysis. We also removed data fitted to the sigmoidal model with $R^2 < 0.70$ from the analysis. Approximately 82% of the 64×53 possible combinations of drug-cell line data passed all of filtering requirements and were used in all of the analyses.

We estimated doubling times for cell lines from the ratio of cell numbers at 72 h to 0 h for untreated cells. We estimated different dose-response parameters for each individual curve, including EC_{50}, IC_{50}, GI_{50}, Hill slope (HS), E_{inf} and E_{max}. In the case of IC_{50} and GI_{50}, when the dose-response data were of high quality, but IC_{50} or GI_{50} values were not reached, we set the values to the largest concentration tested. Additionally, we calculated a parameter AUC representing the area under the relative viability curve, defined as the sum of measured responses (relative viability) at all tested concentrations of the drug. Hence, AUC = 9 corresponds to an inactive compound, whereas smaller AUC values correspond to higher drug activities in inhibiting cell proliferation and/or inducing cell death. When multiple replicates of data on a drug or cell line combination are available, we used medians of the dose-response parameters estimated across replicates for the statistical analysis.

Association of different dose-response parameters with anticancer drugs and breast cell lines. We assessed associations of each of the key dose-response parameters, $\log_{10}(EC_{50})$, $\log_{10}(IC_{50})$, Hill slope, E_{max} and E_{inf}, with the set of $n = 64$ drugs (or $n = 38$ when excluding cell cycle inhibitors) and the set of $m = 53$ cell lines using mutual information[15]. A rationale for using mutual information is to capture differences not only in the median (or mean) but also in the variance of dose-response parameters across different cell lines and compounds. We discretized each of the dose-response parameters X into q equally spaced bins, where $q = $ floor $[\log_2 (\text{no. of samples}) + 1] = 12$ (or $q = 11$ when excluding cell cycle inhibitors)[35]. We defined matrix N for each individual dose-response parameter so that $N_{i,j}$ was the number of cell lines whose dose-response parameter values for the ith drug ($1 \leq i \leq n$) lay within the jth bin of X_d, the discretized form of X ($1 \leq j \leq q$). We computed the empirical mutual information between X_d and the drugs as

$$I(X_d; drugs) = \sum_{i=1}^{n} \sum_{j=1}^{q} P_{i,j} \log[P_{i,j}/(P_i \times P_j)] \quad (2)$$

where

$$P_{i,j} = N_{i,j} / (\sum_{i=1}^{n} \sum_{j=1}^{q} N_{i,j})$$

$$P_i = \sum_{j=1}^{q} P_{i,j}$$

$$P_j = \sum_{i=1}^{n} P_{i,j}.$$

Similarly, we defined matrix M, where $M_{k,j}$ was the number of drugs whose dose-response parameter values for the kth cell line ($1 \leq k \leq m$) belonged to the jth bin of X_d. The empirical mutual information between X_d and the cell lines was given by

$$I(X_d; cell\ lines) = \sum_{k=1}^{m} \sum_{j=1}^{q} P'_{k,j} \log[P'_{k,j}/(P'_k \times P'_j)] \quad (3)$$

where

$$P'_{k,j} = M_{k,j} / (\sum_{k=1}^{m} \sum_{j=1}^{q} M_{k,j})$$

$$P'_k = \sum_{j=1}^{q} P'_{k,j}$$

$$P'_j = \sum_{k=1}^{m} P'_{k,j}.$$

Mutual information scores of zero correspond to independence of the dose-response parameters from the tested drugs and cell lines, whereas larger values imply strong association, indicating that knowing a dose-response parameter value gives important information about drugs and cell lines to which the parameter is expected to belong. To evaluate the significance of the mutual information scores, we computed empirical mutual information P values by randomly shuffling (10,000 trials) the dose-response parameter values among all of the tested cell lines and drugs.

Statistical analysis of drug response profiles. We evaluated differences in values of a dose-response parameter between different drugs or different cell lines by using a nonparametric Wilcoxon signed rank test. We evaluated differences in dose-response parameters between different drug classes that might contain different numbers of drugs by using a nonparametric Mann-Whitney U-test. We corrected P values from the Mann-Whitney U-test and Pearson correlation analyses using the Benjamini-Hochberg method[36] for multiple independent comparisons and the Bonferroni-Holm correction[37] for other comparisons.

To measure the extent of similarity among drug-response profiles, we used pairwise Pearson correlation scores by considering for each drug its pattern of dose-response parameter values across the cell lines. We computed the similarity score for a selected group of N drugs (for example, drugs within a class defined on the basis of drug target or mechanism of action) as the average similarity between all possible pairs of drugs belonging to the selected group (average correlation) divided by the expected average similarity between all possible pairs of drugs in a randomly selected set of N drugs. To evaluate the significance of the similarity score for a selected group of N drugs (SS), we computed empirical P values by permutation test; for a number of $n = 10,000$ trials, we sampled a random set of N drugs from the whole set of 64 drugs and computed the similarity score for that set (SS*). For a given $SS \geq 0$, we counted the number of times (r) that $SS \leq SS*$ across the n permutation trials. We then computed the empirical P value as $(r + 1)/(n + 1)$.

Principal component analysis. Principal component analysis (PCA) is an efficient way to simplify and present multidimensional data into fewer dimensions[38]. For example, each drug in our analysis can be described by 53 IC_{50} values, 53 HS values and 53 E_{max} values corresponding to the parameters for growth inhibition assays for 53 breast cell lines. Therefore, each drug can be represented by a vector pointing into $53 \times 3 = 159$ dimensional space that depicts its effect on the cell line panel. Because it is not possible to visualize 159-dimensional graphs, we used PCA to recognize the 159-dimensional relationships into three primary dimensions (i.e., principal components) that can be plotted on a graph. These principal components are a linear combination of the original dimensions. We organized dose-response parameters into a matrix with 64 rows (corresponding to drugs) and 159 columns (corresponding to dose-response parameters IC_{50}, HS and E_{max} for all cell lines), took the logarithm of parameters, imputed missing values from the nearest-neighbor row (the closest row in Euclidean distance), normalized each parameter value via calculating the Z score for each parameter across the 64 drugs and performed PCA. We can discuss the results of PCA in terms of component scores (the transformed variable values corresponding to a particular data point) and loadings (the weight by which each normalized original variable should be multiplied to get the component score).

Cell lines and reagents. We obtained AU565, HCC1954 and T47D breast cancer cell lines and MCF10A mammary epithelial cells from the American Type Culture Collection (ATCC). We cultured AU565 and HCC1954 cells in RPMI 1640 (ATCC) supplemented with 10% FBS (FBS), T47D cells in RPMI 1640 supplemented with 10% FBS and insulin (0.2 U/ml) and MCF10A cells in DMEM/F12 (Invitrogen) supplemented with 5% horse serum, EGF (20 ng/ml), insulin (10 μg/ml), hydrocortisone (0.5 μg/ml) and cholera toxin (100 ng/ml). We added penicillin (50 U/ml) and streptomycin (50 μg/ml) to all growth medium.

We purchased dactolisib (BEZ235), GSK1059615 and PP242 from Selleck Chemicals. All of the compounds were at least 97% pure, as evaluated by HPLC and MS analysis. All of the compounds were dissolved in DMSO as 10-mM stock solutions. For dose-response experiments, we plated cells in two replicates at 7,000 cells per well in 96-well plates (Corning) in full growth medium for 24 h and then treated them with nine doses in serial dilutions (10^{-10} to 10^{-5} M) of each compound for 6 h, 24 h and 72 h.

Immunofluorescence microscopy. Cells were fixed in 2% paraformaldehyde for 10 min at room temperature and washed with PBS with 0.1% Tween 20 (Sigma-Aldrich) (PBS-T), permeabilized in methanol for 10 min at room temperature, rewashed with PBS-T and blocked in Odyssey Blocking Buffer (LI-COR Biosciences) for 1 h at room temperature. Cells were incubated overnight at 4 °C with rabbit monoclonal antibodies to p-Akt (1:400, Ser473, 4060, Cell Signaling Technology), p-4EBP1 (1:400, Thr37/Thr46, 2855, Cell Signaling Technology), p-S6 ribosomal protein (1:400, Ser235/Ser236, 4858, Cell Signaling Technology), and a goat polyclonal antibody to p-Rb (1:400, Ser807/Ser811, sc-16670, Santa Cruz) in Odyssey Blocking Buffer. Cells were washed three times in PBS-T and incubated with rabbit and goat secondary antibodies labeled with Alexa Fluor 647 and Alexa Fluor 568 (Invitrogen), respectively, diluted 1:2,000 in Odyssey Blocking Buffer. Cells were washed once in PBS-T, once in PBS and then were incubated in 250 ng/ml Hoechst 33342 (Invitrogen) and 1:1,000 Whole Cell Stain (blue; Thermo Scientific) solutions. Cells were then washed twice with PBS and imaged with a 10× objective on Operreta (PerkinElmer). Image segmentation and storage was performed using ImageRail software[39]. Data were analyzed using MatLab software. Selected images were RGB transformed and merged using ImageJ software.

Online databases. Dose-response data (both raw and processed), including estimates of all dose-response parameters used in this study are available online through the Harvard Medical School Library of Integrated Network-based Cellular Signatures (HMS LINCS) database (http://lincs.hms.harvard.edu/db/datasets/20120).

35. Tourassi, G.D., Frederick, E.D., Markey, M.K. & Floyd, C.E. Jr. Application of the mutual information criterion for feature selection in computer-aided diagnosis. *Med. Phys.* **28**, 2394–2402 (2001).
36. Benjamini, Y. & Hochberg, Y. Controlling the false discovery rate: a practical and powerful approach to multiple testing. *J. R. Stat. Soc. Series B Stat. Methodol.* **57**, 289–300 (1995).
37. Holm, S. A simple sequentially rejective multiple test procedure. *Scand. J. Stat.* **6**, 65–70 (1979).
38. Jolliffe, I.T. *Principal Component Analysis* (Springer-Verlag, Berlin, 2002).
39. Millard, B.L., Niepel, M., Menden, M.P., Muhlich, J.L. & Sorger, P.K. Adaptive informatics for multifactorial and high-content biological data. *Nat. Methods* **8**, 487–493 (2011).